Journal of Catalysis **188,** 140–153 (1999)
Article ID jcat.1999.2634, available online at http://www.idealibrary.com on IDEAL®

Oxidation and Redispersion of a Re/γ-Al_2O_3 Catalyst

J. Okal,[1] L. Kępiński, L. Krajczyk, and M. Drozd

Institute of Low Temperature and Structure Research, Polish Academy of Sciences, P.O. Box 1410, 50-950 Wroclaw, Poland

Received April 9, 1999; revised July 5, 1999; accepted July 7, 1999

The interaction of oxygen with rhenium crystallites supported on γ-alumina over a wide temperature range, 20–800°C has been studied. Hydrogen chemisorption, oxygen uptake, and HRTEM, SAED, and XRD methods were applied to monitor morphology changes created upon heat treatment in H_2 and O_2. The structure of the surface rhenium oxide species was determined by HRTEM, Raman spectroscopy, and leaching with the cold water. The results obtained allowed us to propose a detailed mechanism of the oxidation and redispersion of Re crystallites on alumina. At 20–150°C dissociative chemisorption of oxygen occurs with the possible formation of a superficial Re oxide. At 200–300°C the process of oxidation of Re accelerates, with instantaneous sublimation of Re_2O_7 and its simultaneous adsorption as the ReO_4 species on γ-alumina. Metallic Re is still observed in this temperature range. At 400–600°C, the ReO_4 species on the support form two kinds of a surface compound exhibiting Al–O–ReO_3 and Al–(O–ReO_3)$_3$ structures. At 800°C the surface aluminium perrhenate decomposes and a part of the Re oxide sublimes as Re_2O_7. The redispersion of rhenium was observed after H_2 treatment of the oxidized rhenium catalyst. © 1999 Academic Press

Key Words: **Re/γ-Al_2O_3 catalyst; rhenium oxidation; Re_2O_7; redispersion; HRTEM; hydrogen adsorption; Raman spectroscopy.**

INTRODUCTION

Supported rhenium catalysts have been studied extensively for at least two reasons: rhenium in the oxidized state is a very active and selective metathesis catalyst (1, 2) and rhenium in the bimetallic Pt–Re/γ-Al_2O_3 catalyst is the most widely used catalyst in the naphtha reforming (3). The activation or rejuvenation of this different type of catalyst generally includes an oxidation/calcination treatment at 400–600°C. During the regeneration procedure, oxygen treatment removes contamination and causes distinct structural and morphological changes of the catalysts. Oxidation of the Pt–Re/γ-Al_2O_3 catalyst at temperatures above 300°C causes segregation of Pt and Re (3, 7–10). Regeneration of the spent (reduced) Re_2O_7/Al_2O_3 catalyst by oxidation at elevated temperatures leads to the redispersion of rhenium crystals and the formation of a monolayer of supported rhenium oxide (11).

[1] To whom correspondence should be addressed. Fax: +48 71 441 029. E-mail: jana@int.pan.wroc.pl.

Although it is accepted that the redispersion of rhenium (11–14) and the formation of the well-dispersed oxide phase involve oxidation of the alumina-supported rhenium as a crucial step, the complete mechanism of the process is still unknown.

A survey of the literature reveals that the interaction between oxygen and the surface of metallic rhenium is a complex process and depends on the temperature, gas pressure, and the surface coverage by oxygen. For low pressure of oxygen ($\sim 10^{-6}$ Torr) it was established for polycrystalline (15–17) and single-crystal (18–21) samples that adsorbed oxygen is completely dissociated at room temperature. At low oxygen coverage (below 0.5 monolayer) there is only one type of chemisorbed oxygen, while for high coverage (between 0.5 and 1) the formation of a superficial oxide layer was additionally found at room temperature (15–20). Ducros *et al.* (20) demonstrated by XPS that this surface oxide had a thickness of about 2 Å and the composition between Re_2O and ReO. At high temperature, above 1120°C, the surface oxide layer desorbed as ReO_3 and ReO_2 (15, 16). Zaera and Somorjai (22) reported that on a Re film under similar experimental conditions a very stable chemisorption layer of oxygen was formed at −123 to 827°C, with no oxide formation.

The results obtained at low oxygen pressure cannot be directly extrapolated onto Re films, powders, and supported rhenium oxidized under atmospheric conditions. Tysoe *et al.* (23) studied the oxidation of thin Re films deposited on Pt foil at atmospheric pressure and found by XPS that a mixture of rhenium oxides was formed above 200°C and loss of rhenium due to the formation of the volatile Re_2O_7 occurred after treatment above 300°C.

The interaction of oxygen with alumina-supported rhenium at room temperature was studied particularly in connection with the problem of estimation of the metal surface area (7, 14, 24–31), and only a few results refer to oxidation at high temperature (7, 14, 25, 26, 28, 29). It has been established that in the temperature range 20–500°C chemisorption on the surface as well as bulk oxidation of rhenium occur. There is, however, no consensus in the literature regarding the oxidation state of rhenium supported on γ-Al_2O_3. Wagstaff and Prins (7) found from TPR that an average oxidation state of Re is 2 at 100°C, 4 at 180°C, and

0021-9517/99 $30.00

7 at 300°C. Yao and Shelef (14) reported the average oxidation state of Re between +4 and +7 at 500°C. Paryjczak *et al.* (26) distinguished three temperature ranges of different oxygen–rhenium interactions: superficial oxide (30–200°C), bulk oxidation (200–400°C), and above 400°C when ReO_3 is formed. Other studies suggested that at or above 300°C rhenium heptaoxide is the main product of oxidation of Re supported on alumina (3, 7, 14, 29) or rhenium powder (32).

It is well known that Re_2O_7 sublimes above 200°C (33, 34). However, it appears that interaction of Re with γ-alumina support prevents its loss from the catalyst even at high temperature (14). According to the literature, rhenium in an oxidized state on γ-alumina exists always as well-dispersed oxide (11). Crystalline rhenium oxide, Re_2O_7, has never been detected in the calcined Re/γ-Al_2O_3 catalysts by either X-ray diffraction (35–37) or selected area electron diffraction (12, 38). Studies by numerous spectroscopic techniques as IR (11, 37, 39–42), laser Raman (4–6, 43, 44), ESR (45, 46), XPS (47–49), and NMR (50) supported this observation and gave evidence that, even at high loading, the rhenium oxide is monomolecularly dispersed on the alumina surface, as ReO_4^- tetrahedra. Recently, Vuurman *et al.* (4, 5) have shown by *in situ* Raman spectroscopy, IR, and TPR that two slightly different surface rhenium oxide species are present on the alumina at high surface coverage.

The nature and mechanism of formation of the Re–oxide phases occurring during the oxidation of supported rhenium is still under debate. Therefore, we undertook a detailed investigation of the microstructure changes of the Re/γ-Al_2O_3 catalyst on activation both in H_2 and O_2 at 20–800°C. On one hand, a high loading of 10.4 wt% Re, which is significantly higher than that used in a reforming catalyst (0.3% Re–0.3% Pt/Al_2O_3), was chosen so that high-resolution electron microscopy (HRTEM) and selected area electron diffraction (SAED) could be effectively used to study the state of Re after treatments. On the other hand, high loading of Re is necessary to obtain an active and highly selective metathesis catalyst (4, 5). The molecular structure of the oxide phase was determined by Raman spectroscopy and a chemical method of Re extraction with cold water.

EXPERIMENTAL

1. Preparation and Treatment

The Re/γ-Al_2O_3 (10.4 wt%) catalyst was prepared by impregnation of γ-alumina (BET area 220 m^2/g) with an aqueous solution of ammonium perrhenate. The support was prepared in another laboratory by hydrolysis of aluminum isopropoxide followed by calcination at 500°C to obtain γ-Al_2O_3 (51). After impregnation the sample was dried in air at 100°C for 24 h and then reduced in hydrogen flow (with a heating rate of 6°C/min) at 550°C for 10 h (12). Next, the sample underwent the following sequential heat treatment procedures.

Sintering. The catalyst was again reduced in flowing hydrogen with a heating rate of 6°C/min from room temperature to 550°C, held at this temperature for 20 h, and then reduced at 800°C for 5 h. After cooling to room temperature, the catalyst was exposed to air, closed in a glass vessel, outgassed to 10^{-2} Torr (1 Torr = 133 N/m^2), and stored until characterization.

Oxidation. The sintered sample was oxidised with static air at temperatures of 20–800°C. The samples were heated from room temperature to the desired one at the rate of 5°C/min, held at this temperature for 1 h (up to the temperature of 500°C) or 4 h at 600, 700, and 800°C.

Redispersion. The sample of the sintered catalyst was oxidized in air at 500°C for 1 h and then reduced in flowing hydrogen at 550°C for 20 h.

2. Experimental Techniques

Adsorption methods. In all adsorption experiments a glass apparatus equipped with a conventional high vacuum system (base pressure 10^{-6} Torr) was employed. The amount of adsorption was determined volumetrically.

For hydrogen chemisorption, the catalyst sample (ca. 0.2 g), after being outgassed at room temperature, was subjected to repeated heating at 500°C in H_2 at 200 Torr for 2–4 h and then at the same temperature under vacuum for 2 h. Finally, after evacuation at 500°C, the sample was saturated with H_2 at 150 Torr from 500°C to room temperature. The time needed for cooling the sample was about 3 h. The amount of irreversibly bound hydrogen was used to calculate the dispersion of Re, assuming 1 : 1 stoichiometry of H : Re (29).

The oxygen uptake was measured at 20–500°C with the oxygen pressure of 100–150 Torr. The reduced sample (ca. 0.1 g) was pretreated *in situ* in H_2 at 500°C for 2 h, outgassed at the same temperature for 2 h, and cooled under dynamic vacuum to room temperature. Then, oxygen was introduced and the amount of total adsorbed oxygen was measured. The temperature was subsequently raised to the desired oxidation temperature, at the rate of 5°C/min, kept in isothermal conditions for 1 h, and then was cooled under oxygen to room temperature, where the uptake was measured. Fresh sample was used for each oxidation experiment.

The BET surface area of the support and the catalyst were measured by nitrogen adsorption at liquid nitrogen temperature, assuming 0.162 nm^2 as the area of the adsorbate molecule.

Structure studies. XRD spectra were obtained with the STOE powder diffractometer equipped with a position-sensitive detector and operated with monochromatised Cu $K\alpha$ radiation.

HRTEM and electron diffraction (SAED) studies were carried out with a Philips CM 20 microscope equipped with the SuperTwin objective lens ($C_S = 1.2$ mm) and operated at 200 kV. Specimens for TEM were prepared simply by dipping a copper microscope grid covered with holey carbon film in the freshly prepared sample.

The Raman spectra were measured with a Jobin-Yvon Ramanor-U1000 spectrometer equipped with the CCD detector cooled to −130°C. The 514.5-nm line (power of 150 mW) of the Ar^+ ion laser was used as an exiting light. The resolution was ca. 2 cm^{-1}. The spectra were measured at room temperature, 30-s time exposition being applied. The samples were kept in the sealed capillaries to avoid contact with air.

3. Chemical Analysis

The weight percentage of Re in the catalyst was calculated from the amount of ammonium perrhenate used for the impregnation. Additionally, the rhenium content was measured by inductively coupled plasma-atom emission spectrometry (ICP-AES) with a Philips Scientific PU 7000 spectrometer (the 228.751-nm line of rhenium was used), according to the procedure given in (52).

Extraction of rhenium and aluminium by cold deionized water from the calcined samples was performed by the method described recently by Schekler-Nahama *et al.* (53).

RESULTS

1. Chemical Analysis

Basic characteristics of the 10.4 wt% Re/γ-Al_2O_3 catalyst subjected to various treatments are presented in Table 1. Oxidation at temperatures up to 600°C did not change the Re content in the catalyst; however, at 800°C part of the rhenium (33%) left the surface of the catalyst as gaseous Re_2O_7. Deposition of Re_2O_7 was detected on the colder parts of the quartz reactor tube. Additionally, from Table 1 it appears that the alumina support undergoes textural changes upon reduction at 800°C, with some loss of the surface area which may be responsible for some sintering of Re.

TABLE 1

BET Surface Area and Re Content (wt%) for 10.4 wt% Re/γ-Al_2O_3 Catalyst after Various Heat Treatments

Reduction (°C)	Oxidation (°C)	BET surface area (m^2/g)	Re content (wt%)
550	—	230	10.6
550	400	230	10.7
800	—	153	—
800	600	153	10.0
800	800	151	7.0

2. Structure Characterization

Figure 1 shows the HRTEM image of the sintered Re/γ-Al_2O_3 catalyst (the SAED pattern is included as an inset). Dark particles with sizes of 4–10 nm exposing sharp, well-developed crystal faces and lattice fringes with spacings of 0.222 and 0.212 nm are seen on the support. The fringes are generally parallel with no indication of twinning or stacking faults, implying that the particles are single crystals. High contrast produced by the particles and spacings of the lattice fringes allow one to identify the particles as metallic rhenium. The γ-alumina support is polycrystalline with grains exposing flat crystal faces of a few nanometers in size. In the SAED pattern (see inset) continuous rings and individual spots are present. *d* values calculated from the pattern are collected in Table 2 and compared with those of the Re and γ-Al_2O_3 standard samples. Continuous rings correspond well with the strongest lines of γ-Al_2O_3, while spots situated between γ-Al_2O_3 (400) and (311) rings may be ascribed to metallic Re (002) and (101) crystal planes. Since most of the Re and γ-Al_2O_3 lines overlap, only Re (101) can safely be used to the metal identification. Table 2 contains also data for various rhenium oxides, which could possibly form during oxidation of Re/γ-Al_2O_3 samples. In this case, however, only the strongest lines are given.

Figure 2 shows HRTEM images of Re/γ-Al_2O_3 samples oxidized at 200°C (a) and 250°C (b). Two fractions of particles are present on the support: well-developed crystallites with sizes up to 8 nm and very small particles (∼0.6 nm) uniformly distributed on γ-Al_2O_3. Lattice fringes measured on large crystallites (0.212 and 0.222 nm) fit to metallic Re. We never observed on such particles fringes with spacings bigger than 0.24 nm, which should occur if the particles would consist of any Re oxide (cf. Table 2). The identification of the small particles cannot be done by HRTEM or SAED since they are too small to exhibit lattice fringes or visible diffraction features. An approximate concentration of the small particles on the support is 1 particle/8 nm^2 and the particles seem to be located preferentially at special sites on alumina such as edges and corners (Fig. 2b). SAED patterns of the samples presented in Fig. 2 (not shown) were very similar to those in Fig. 1, i.e., only continuous alumina rings and spots from metallic Re were present with no indication of any Re oxide. The absence of any oxide layer on Re particles is also clearly seen in Fig. 2b. To check this point further, we performed an additional experiment with Re black oxidized at 150°C. Clear, sharp faces of Re crystallites with no sign of an oxide layer were observed in the HRTEM and only Re diffraction rings were present in the SAED pattern.

In the sample oxidised at 300°C a number of Re particles decreased drastically, but we still could find some small crystallites. An example is shown in Fig. 3a, where two Re crystallites are seen. A magnified image of one crystallite is presented in Fig. 3b, together with its fast Fourier

TABLE 2

Interplanar Spacings *d*(nm) and Intensities of Crystal Phases Measured from SAED Pattern and XRD Data for Crystal Phases Possibly Occurring in the Samples Studied

Observed			Re[a]			γ-Al_2O_3[b]		ReO_2[c]		ReO_2[d]		Re_2O_7[e]		ReO_3[f]	
d	*I*	*hkl*	*d*	*I*	*hkl*	*d*	*I*	*d*	*I*	*d*	*I*	*d*	*I*	*d*	*I*
					111	0.465	40								
								0.366	100	0.340	100	0.382	100	0.376	85
					220	0.280	20	0.286	100						
												0.254	40	0.265	80
0.241	m.	100	0.239	32	311	0.239	80	0.240	80	0.240	100				
0.220	s.p	002	0.223	34	222	0.228	50	0.230	80						
0.210	s.p	101	0.210	100						0.214	40			0.217	25
0.199	s				400	0.198	100	0.195	80			0.191	36	0.188	50
								0.170	100					0.168	100
		102	0.163	11				0.166	80						
					511	0.152	30	0.154	50	0.152	40	0.153	18	0.153	55
0.140	s	110	0.138	22	440	0.139	100	0.141	50	0.138	30			0.133	30

[a] JCPDF File 5-702.
[b] JCPDF File 10-425.
[c] JCPDF File 9-274.
[d] JCPDF File 17-600.
[e] JCPDF File 39-934.
[f] JCPDF File 33-1096.

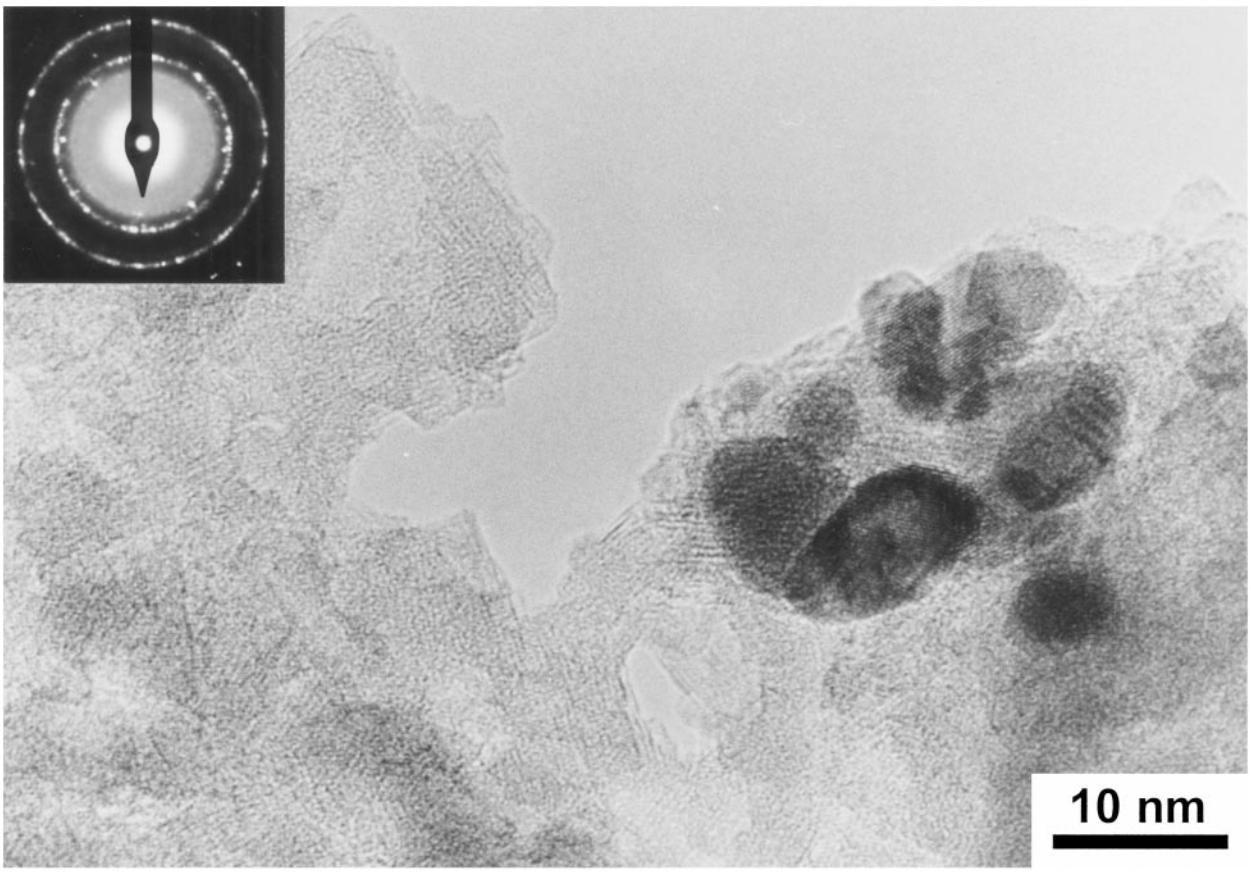

FIG. 1. HRTEM image and SAED pattern (inset) of 10.4 wt% Re/γ-Al_2O_3 sintered by reduction at 800°C. The lattice fringes on dark particles correspond to metallic Re.

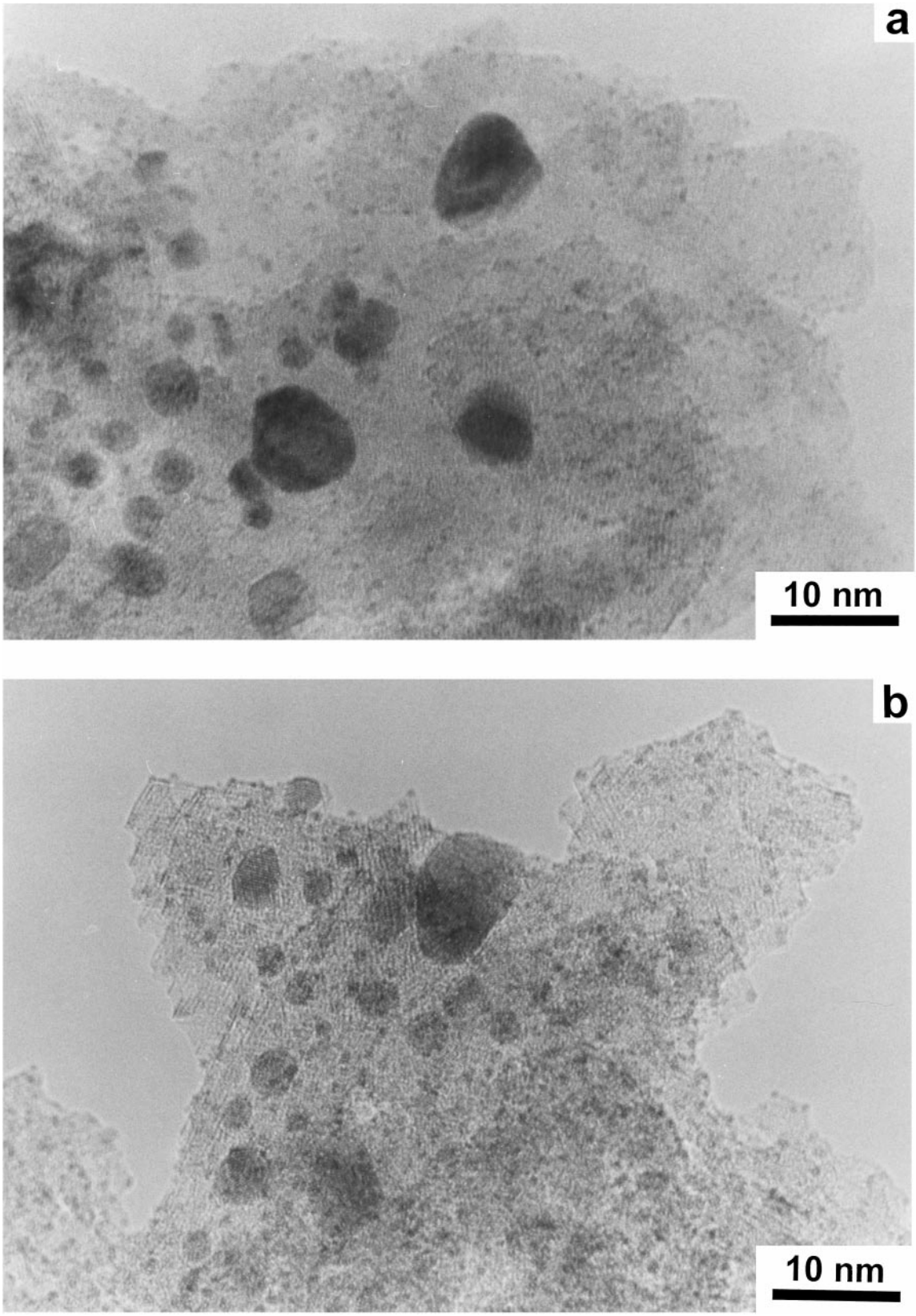

FIG. 2. HRTEM images of the sintered catalyst oxidised at 200°C (a) and 250°C (b). Bigger, dark particles are metallic Re; small (~0.6-nm) particles originate from the surface Re–O phase.

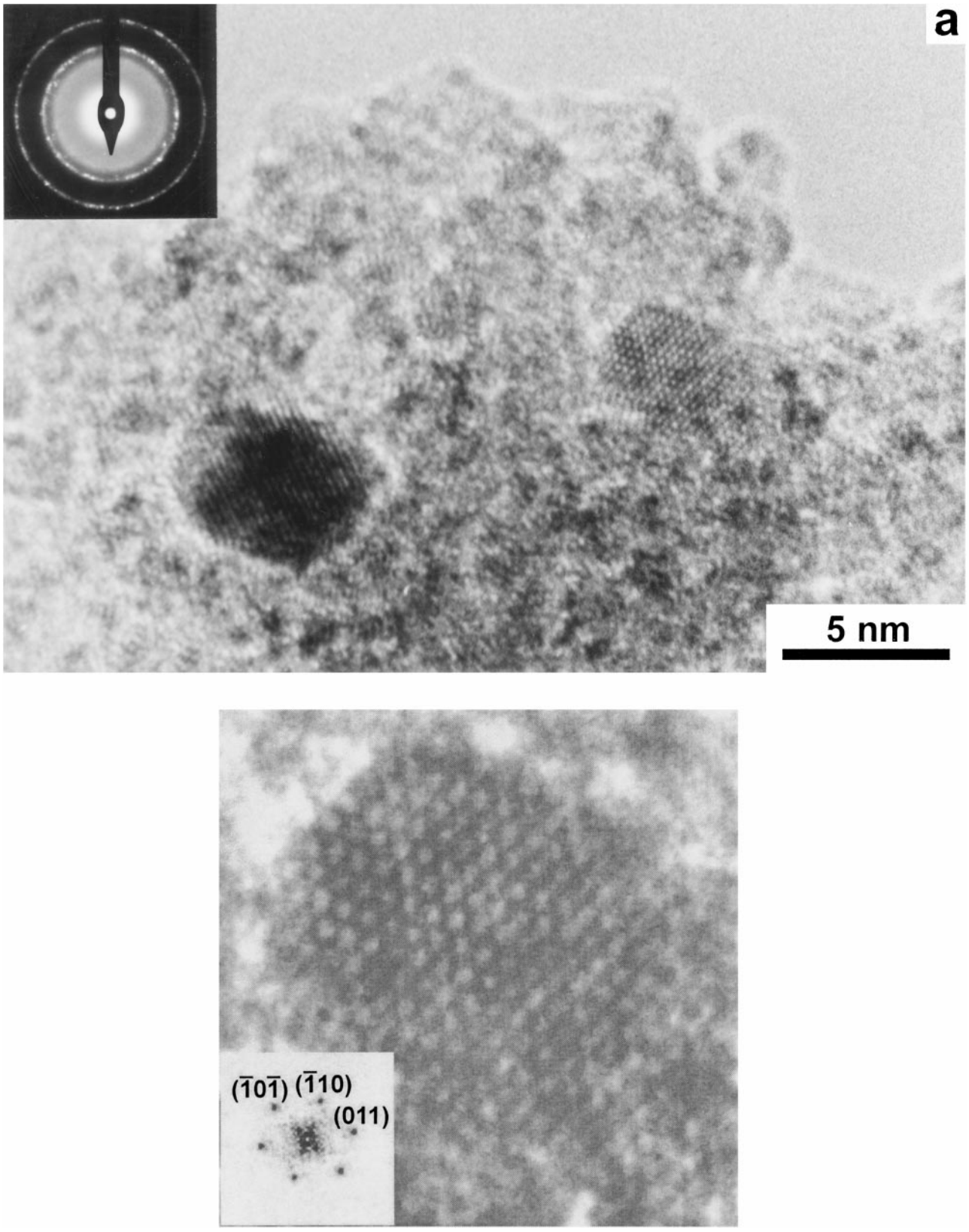

FIG. 3. HRTEM image and SAED pattern (inset) of the catalyst oxidised at 300°C (a) and magnified image of the Re crystallite with its FFT pattern (b).

transform (FFT). The FFT could be indexed as hexagonal Re in the [111] orientation. In the SAED pattern taken from the sample (inset in Fig. 3a), weak spots of metallic Re are also present.

In samples oxidized at or above 400°C, no metallic Re could be detected by HRTEM and SAED. Figure 4 shows an HRTEM image of the catalyst oxidised at 600°C (a) and 800°C (b). In both images the fraction of small particles is clearly visible. The size of the particles increased in comparison with the sample oxidised at 250°C (Fig. 2a), to ~1 nm at 600°C (Fig. 4a), and then again decreased to ~0.6 nm at 800°C (Fig. 4b). However, no visible change in the concentration of the particles could be seen. The SAED pattern from the sample oxidised at 600 and 800°C were identical and contained only lines of γ-Al_2O_3 (see inset in Fig. 4a).

Figure 5 shows an HRTEM image and SAED pattern (inset) of the catalyst subjected to the redispersion procedure (reduction at 550°C of the sample oxidised at 500°C). Reappearance of metallic particles with sizes up to 8 nm is evident. Lattice fringes observed on the particles (0.212, 0.223, and 0.239 nm) can be ascribed to metallic Re. In the SAED pattern weak diffraction spots from Re are also present (cf. Fig. 1). In Fig. 6 distributions of Re particle size in the sintered and redispersed samples are shown. The total number of particles measured in both cases was about 700 and the mean particle size calculated from the histograms was 4.9 and 1.6 nm, respectively. It is worth mentioning that in addition to a 3-fold decrease of the mean particle size the redispersion procedure also caused more uniform distribution of Re particles on the support (cf. Figs. 1 and 5). XRD studies confirmed the results obtained by electron microscopy. In the sintered sample only lines of γ-Al_2O_3 and metallic Re were present with no indication of phase transformation of alumina support to high-temperature δ or α phases. The mean Re crystallite size determined from the half-breath of the Re reflection (by the Scherrer formula) was 5.9 nm. In the redispersed sample reflections from Re could not be seen in the XRD spectra due to the small size of Re crystallites.

TEM observations of the sample subjected to the "extraction" procedure revealed that the Re species left on the γ-Al_2O_3 support and calcined at 600°C form very small dark particles similar to those observed in Fig. 4a. An average size of the particles is, however, smaller (~0.5 nm). In the HRTEM images of the residue left after evaporation (at 200°C) of the solution used to extract Re species from the oxidised sample, we found very fine crystalline solids with broad SAED rings that could be ascribed to γ-Al_2O_3.

3. Chemisorption of Hydrogen

Table 3 shows data on the dispersion of rhenium (D) in the Re/γ-Al_2O_3 catalyst subjected to various heat treatments. The metal particle size determined from H_2 chemisorption is compared with TEM and X-ray diffraction results. Dispersion of rhenium decreased by 36% after increasing the reduction temperature from 550 to 800°C, in good agreement with our earlier data (54). The average particle size of rhenium in the sample reduced at 800°C (5.4 nm) agrees well with the values obtained by TEM and XRD, indicating sintering of Re. Heating of the sintered sample in oxygen or in air at 500°C for 1 h followed by reduction in hydrogen at 550°C resulted in the redispersion of rhenium. Small Re particles with an average size of 1.9 nm were obtained by this procedure. TEM, XRD, and H_2 chemisorption results were again in good agreement.

TABLE 3

H_2 Chemisorption Data and Metal Particle Size of 10.4 wt% Re/γ-Al_2O_3 Catalyst after Various Treatments

Treatment T(°C)/time/gas	H_2 chemisorption μmol g^{-1} cat.	D^a	l (chem.)^b	l (TEM)^c	l (XRD)^d
550/20 h/H_2	109.0	0.39	3.4	—	—
+ 800/5 h/H_2	70.0	0.25	5.4	4.9	5.9
+ 500/1 h/O_2 + 550/20 h/H_2	199.0	0.71	1.9	1.6	n.m.

[a] Dispersion of Re, number of hydrogen atoms chemisorbed to the total number of Re atoms (H/Re).

[b, c, d] Metal particle size (nm) determined from H_2 chemisorption, TEM, and XRD, respectively.

4. Uptake of Oxygen

The uptake of oxygen (in μmol per 1 g of catalyst) by the sintered Re/γ-Al_2O_3 catalyst as a function of the oxidation temperature is presented in Fig. 7. The O/Re values given in Fig. 7 denote the ratio of the number of adsorbed oxygen atoms to the total number of Re atoms in the catalyst. Oxygen uptakes at 20 and 150°C are low and corresponed to dissociative chemisorption (15–21). The coverage of the rhenium surface with oxygen equal to 0.64 (expressed as O/H) is comparable with the literature data (18, 19, 21, 26, 29, 55). Difficulties in obtaining the saturation of the Re/γ-Al_2O_3 catalysts with oxygen may be caused by some penetration of oxygen into the subsurface region of rhenium (20, 29).

Oxygen uptakes increased gradually on raising the oxidation temperature and attained a maximum level at 300–500°C. The O/Re ratio amounts to 3.3 which is only 6% lower than the 3.5 value corresponding to the complete oxidation of Re to rhenium heptaoxide, Re_2O_7. The volatization of rhenium heptaoxide was not observed at such temperatures (see Table 1) and could not be responsible for the underestimation of the O/Re ratio. However, it is possible that a small part of gaseous Re_2O_7 formed upon

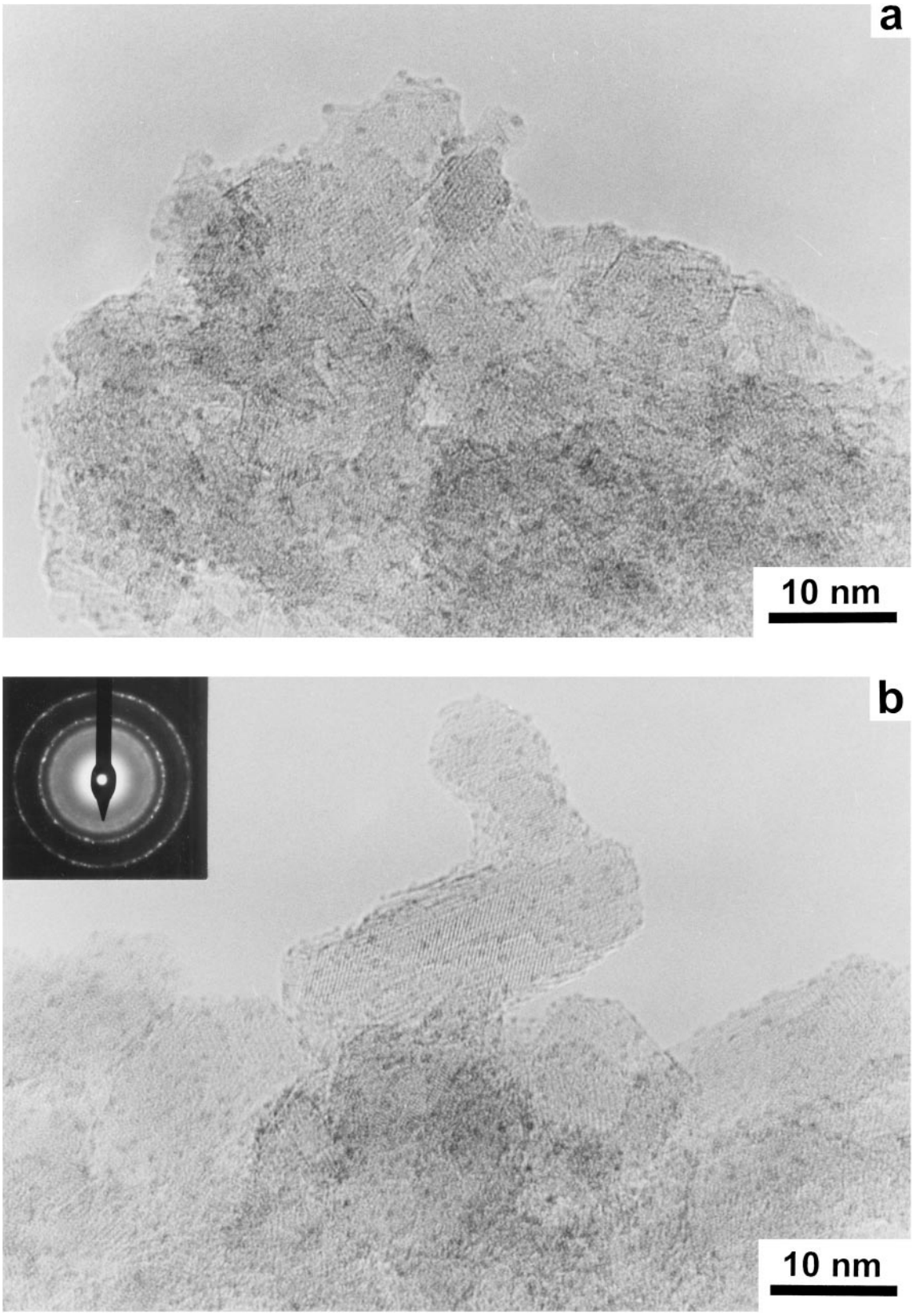

FIG. 4. HRTEM images and SAED pattern (inset) of the catalyst oxidised at 600°C (a) and 800°C (b). Note the small, dark particles (~1 nm) located at the edges and corners of the support.

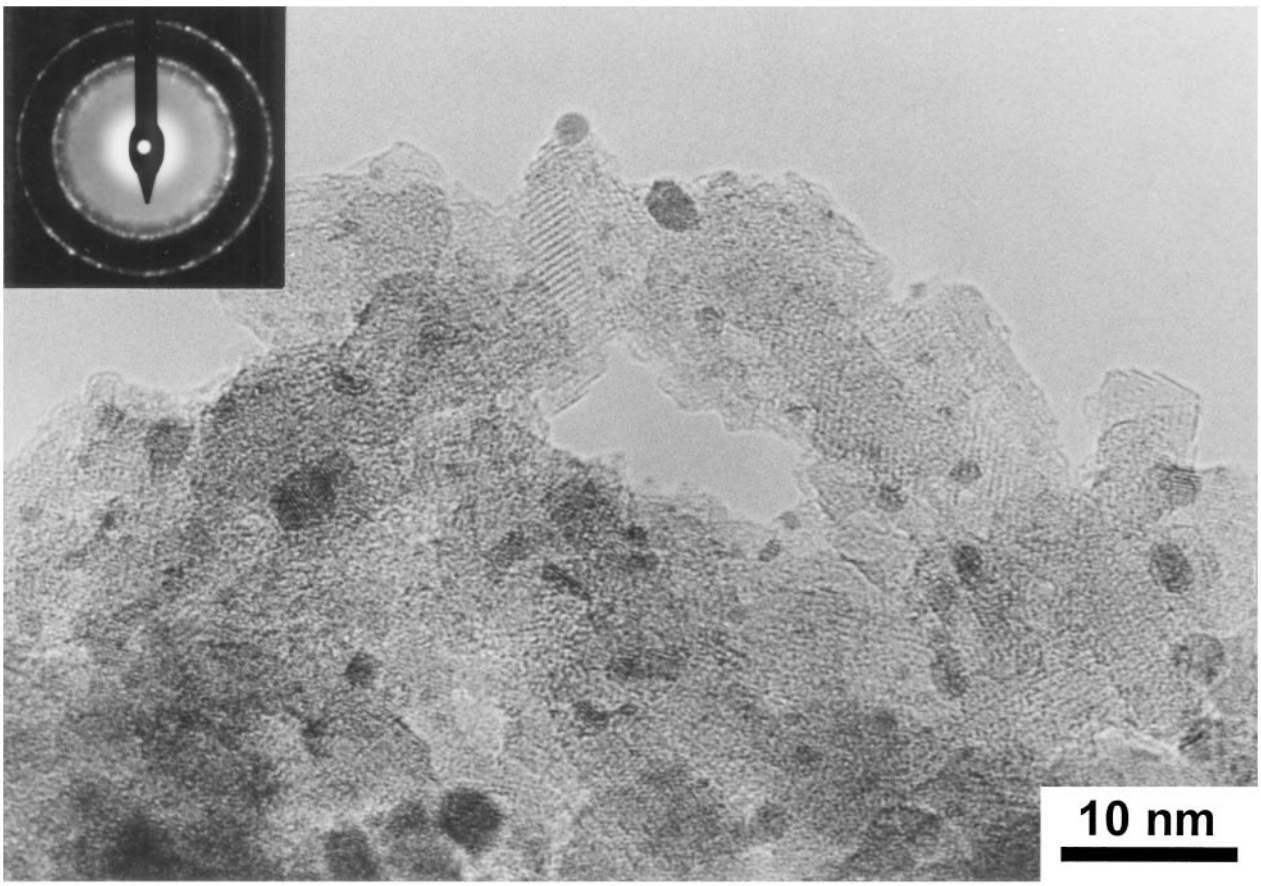

FIG. 5. HRTEM image and SAED pattern of the redispersed catalyst. Note the smaller size and more uniform distribution of Re particles.

oxidation above 300°C undergoes thermal decomposition to ReO_2 with the liberation of oxygen (33).

The colour of the catalyst samples turned from black (due to Re^0) after oxidation at 20–150°C, to gray at 300°C, and then to white above 500°C. This change indicated a successive rise of the average oxidation state of rhenium. The exact oxidation state of Re at a given temperature is, however, generally uncertain.

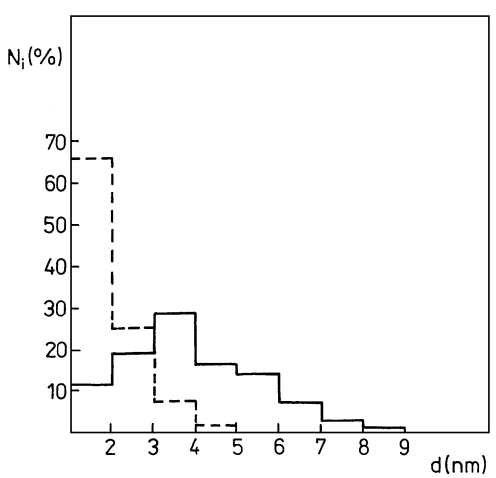

FIG. 6. In the size distribution of the 10.4 wt% Re/γ-Al_2O_3 catalyst before (—) and after (- - -) redispersion. Average particle size calculated from the distributions is 4.9 and 1.6 nm, respectively.

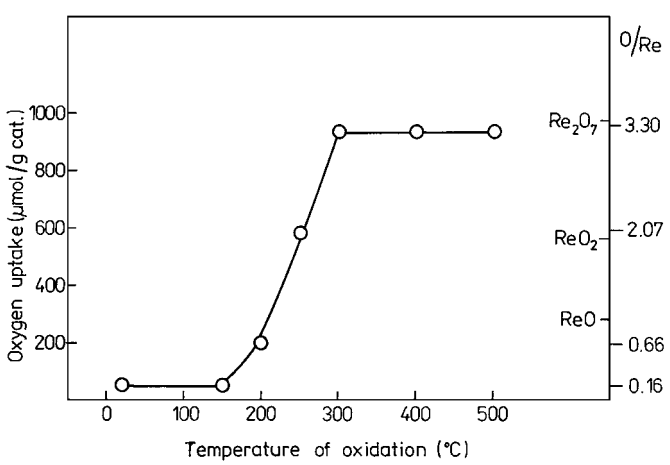

FIG. 7. Oxygen uptake measured as a function of the oxidation temperature for the sintered 10.4 wt% Re/γ-Al_2O_3 catalyst. Formal Re–O stoichiometry corresponding to the measured uptakes is given for comparison.

TABLE 4

Amounts of Re and Al Extracted from the Calcined 10.4 wt% Re/γ-Al_2O_3 Catalyst (Measured by the ICP-AES Method)

Calcination (°C)	Re_{extr}[a] (%)	Re in solution (mol Re/L)	Al in solution (mol Al/L)	Re/Al molar ratio
400	43.1	9.6×10^{-3}	3.5×10^{-3}	2.7
600	50.4	11.3×10^{-3}	5.2×10^{-3}	2.2
800	55.7[b]	8.3×10^{-3}	8.0×10^{-3}	1.0
600[c]	—	—	8.5×10^{-4} [c]	—
600[d]	—	10.8×10^{-3} [d]	5.7×10^{-4} [d]	19.0

[a] $Re_{extr.}$ (%) = Re in the extraction solution/g cat./Re on the catalyst before extraction $\times 100$.
[b] Corrected for 33% loss of Re upon oxidation at this temperature.
[c] Solubility of bare γ-alumina.
[d] Solubility of bare γ-alumina in $HReO_4$ aqueous solution.

5. ReO_4^- Extraction Experiments

Some knowledge about the nature of species formed upon oxidation of alumina-supported rhenium can be drawn from water leaching of the oxidized catalyst (53). As seen from Table 4 the amount of rhenium extracted from the catalyst increases with the calcination temperature. Moreover, we found significant aluminium concentration in the extraction solution which indicates the enhanced solubility of γ-alumina as compared with that of the bare support. The pH of the leaching solution of the calcined Re/γ-Al_2O_3 catalyst was about 4. In a separate experiment we determined also the extraction of Al from bare γ-alumina into the solution of $HReO_4$. The concentration of ReO_4^- ions in solution, initial pH, and initial contact time (4 h) were similar to that applied in the extraction experiment for the catalyst sample. As appears from Table 4 the amount of extracted Al was equal, within the experimental error, to that for bare γ-alumina extracted in pure water. This result demonstrates that the presence of ReO_4^- ions, i.e., of anions of a strong acid, in solution is not enough to cause the substantial increases of the solubility of the γ-alumina.

Schekler-Nachama *et al.* (53) showed, moreover, that rhenium and aluminium were extracted together from Re_2O_7/γ-Al_2O_3 calcined at 550°C with a (Re/Al) molar ratio of 3, corresponding to the Re/Al stoichiometric ratio in aluminium perrhenate, $Al(ReO_4)_3$. $Al(ReO_4)_3$ is a white-coloured substance, is well soluble in water, and decomposes in air above 300°C (57). We obtained the (Re/Al) molar ratio close to 3 only for the sample calcined at 400°C, and at higher calcination temperatures the molar ratio decreased (Table 4). If we assume that a surface aluminium perrhenate is formed upon the calcination of the Re/γ-Al_2O_3 catalyst, the decrease in the Re/Al molar ratio may point to some decomposition of this salt. After partial loss of Re, upon calcination at 800°C, Al^{3+} ions initially participating in the surface compound can easily be extracted (53). We want to stress, however, that the results, particularly those of the aluminium concentration in water solutions, should be considered with some caution. The analysis was difficult because we obtained a slightly turbid solution after extraction of Re and Al from the catalyst. The reason was probably precipitation of a coloidal aluminium hydroxide.

6. Raman Studies

The Raman spectra of the 10.4 wt% Re/γ-Al_2O_3 catalyst calcined in air at 600°C for 4 h are presented in Fig. 8. The Raman bands between 920 and 1015 cm^{-1} are assigned to the terminal Re=O stretching vibration and those between 337 and 343 cm^{-1} to the O–Re–O bending mode of the surface oxide species (4, 5).

Spectrum A originates from the sample without contact with atmospheric moisture. The spectrum exhibits Raman bands at 1015, 1006, 980, and 343 cm^{-1}, which according to literature can be ascribed to two slightly different surface rhenium oxide species present on alumina under dehydrated conditions (4, 5). One species was observed at all coverages of rhenium and showed bands at 1004, 890, and 340 cm^{-1}, while a second one was present at higher loadings only and produced bands at 1015, 980, and also 340 cm^{-1}. The structure of the species is similar; both possess three terminal Re=O bonds and one bridging Re–O–support bond (4, 5). In the present study we did not observe a weak, broad band at 890 cm^{-1}, which is assigned to the antisymmetric stretching modes of the first rhenium oxide species. The second rhenium oxide species has a weaker Re–O–support bond what was established by TPR measurement (5). As a consequence, the terminal Re=O bonds are stronger, which explains the shift of the Raman band of ν (Re=O) to higher frequency (1015 instead of 1006 cm^{-1}).

Spectrum B was taken from the sample after 20 h of contact with atmospheric moisture. The main Raman bands shift from 1015 and 1006 cm^{-1} to 995 and 975 cm^{-1} and from 343 to 338 cm^{-1}, respectively. The shift of the bands to lower frequencies is caused by the partial hydrolysis of the Re–O–Al bonds, created during calcination at 600°C. The two bands at 995 and 975 cm^{-1} are still present, so that two different surface rhenium oxide species can be differentiated.

Raman spectrum C was measured for the sample that was exposed to atmospheric moisture for a few days after calcination. Three bands observed at 974, ~920, and 337 cm^{-1} correspond to the Raman spectrum of the ReO_4^- species in an aqueous solution (44).

Spectrum D is from the sample subjected to water leaching and then dehydrated at 600°C for 4 h. Only one surface rhenium oxide species is observed which exhibits a single, sharp band at 1003 cm^{-1} and a weak band at 342 cm^{-1}. Probably, a second surface rhenium oxide species (bands at 1015, 980, and 343 cm^{-1}) has been extracted from the catalyst due to weaker interaction with the alumina support. No one Raman spectrum presented in this study shows the

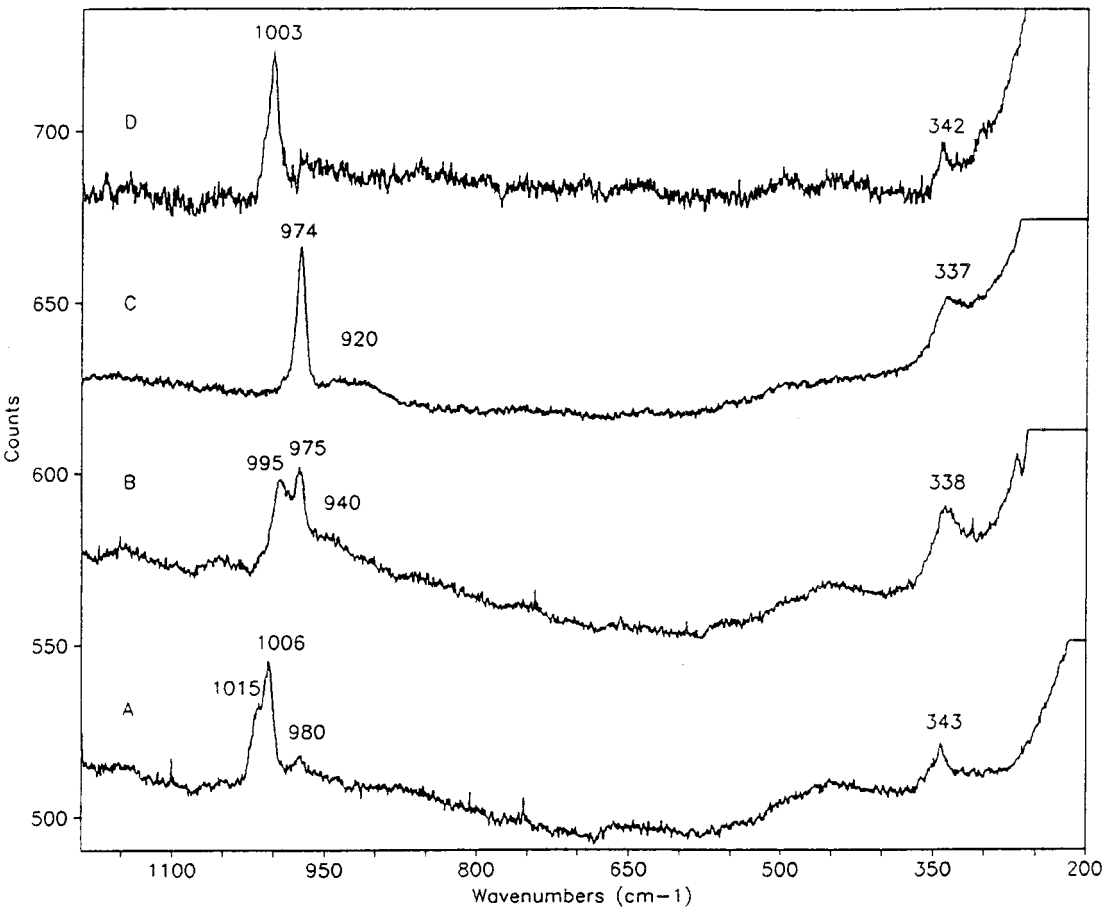

FIG. 8. Raman spectra recorded for the catalyst oxidised at 600°C: no contact with laboratory air (A), exposure to ambient conditions for 20 h (B), exposure to ambient conditions for a few days (C), and subject to extraction procedure followed by oxidation at 600°C (D).

strong Re–O–Re vibrations (at ~450 cm^{-1} and in the 200- to 150-cm^{-1} region), which indicates that lateral interaction between rhenium surface species are absent in the samples.

DISCUSSION

In discussion of the results obtained by HRTEM we have to focus on the problem of identification of the highly dispersed phase observed in the images of samples oxidised at or above 150°C. Considering the conditions of the formation of this phase, we have to assume that it constitutes oxidised rhenium, most probably in the form of the $(ReO_4)^-$ species. The volume occupied by a $(ReO_4)^-$ tetrahedron can be estimated from crystal data for Re_2O_7 (56) as 65 $Å^3$. Assuming a hemispherical shape of the dark spots in the HRTEM images and radius of 5 Å (maximum value), we obtain the volume of ~260 $Å^3$. It means that one such particle could contain a maximum 4 $(ReO_4)^-$ tetrahedra. Since the average density of the particles on the support is 1 particle/8 nm^2, we obtain an estimation of 1 $(ReO_4)^-$ tetrahedron/or 1 Re^{7+} ion/2 nm^2. This value is much too small when compared with the actual surface coverage of 1 Re ion/0.45 nm^2 calculated from the metal loading (10.4 wt%) and surface area of the alumina support (151 m^2/g). We have therefore to assume that not all of the Re–O phase is visible in HRTEM micrographs, probably due to its dispersion as individual $(ReO_4)^-$ species. The dark spots could possibly be aggregates of $(ReO_4)^-$ tetrahedra grouped around special sites on γ-Al_2O_3, e.g., as $Al(ReO_4)_3$ species. A chemical compound with the stoichiometry $Al(ReO_4)_3$ has been synthesised by Baud and Capeston (57) but its structure is unknown. In the bulk form the compound starts to decompose in air at 350°C into Al_2O_3 and Re_2O_7. In a recent paper on Mo/γ-Al_2O_3 Peeters *et al.* (58) reported that in the oxidised sample even at monolayer coverage (1 Mo atom/0.33 nm^2) the Mo containing phase is invisible in the HRTEM. At higher coverages, however, quite large (>20 nm) crystallites identified as orthorhombic $Al_2(MoO_4)_3$ were observed by HRTEM and XRD (58).

Another possible interpretation of the HRTEM images of the oxidised samples assumes that the small dark particles with sizes below 1 nm are Re clusters formed inside the electron microscope (vacuum) under the influence of the electron beam. A crude estimation shows that in such

a case one particle with a diameter of 1 nm could contain 17 Re atoms and we obtain 1 Re atom/0.47 nm^2 of γ-Al_2O_3 surface, in good agreement with the value calculated from the metal loading. This interpretation is in line with that of Reardon *et al.* (59) who observed by HRTEM very small (1-nm) particles in oxidised Mo/γ-Al_2O_3 and stated that they grow under the electron beam due to the decomposition of the $(MoO_4)^{-2}$ species. To check this hypothesis, we recorded HRTEM images of our sample oxidised at 600°C after 5 and 10 min of exposure to an electron beam, but no measurable change in the particle size or position could be observed. It means that in the case of the $(ReO_4)^-$ species on γ-Al_2O_3 their decomposition and aggregation of Re atoms should occur already at very small exposure times (during focusing of the sample).

Some insight into the molecular structure of the surface rhenium oxide species supported on γ-alumina can be gained from the Raman spectra. It should be noted, however, that the spectra depend on the degree of the hydroxylation of the catalyst, as is shown by the present results, which are in line with recent data of Kim and Wachs (6). Under ambient conditions the surface rhenium oxide species is hydrated by adsorbed moisture and is essentially in an aqueous medium. Hence, an isolated ReO_4 structure similar to the structures present in an aqueous solution is observed on the surface of the catalyst. Under dehydrated conditions, two slightly different surface rhenium oxide species are present on γ-alumina. It has been proposed by Turek *et al.* (40) that the slight difference between the two surface rhenium oxide species may be due to the distortions brought about by the presence of a proton on the Re–O–support bond of one of the rhenium species. This causes the shift of the Raman band of the terminal Re=O bond from 1006 to 1015 cm^{-1}. Such a shift of the frequency can also be interpreted as a weakening of the bridging Re–O–Al bond strength.

The surface oxide species with weaker interactions with the support may be extracted from the catalyst surface more easily by washing with cold water. The amount of Re extracted from the catalyst increased slightly with the temperature of oxidation, indicating that the amount of the rhenium oxide species with weaker interactions with the support also increases.

It is known from the literature (60) that most of the rhenium can be removed by cold water treatment from the catalyst prepared by the equilibrium adsorption method which was only dried at room temperature. However, as found by Edreva-Kardijeva and Andreev (37), calcination at 550°C of the 13 wt% Re_2O_7/Al_2O_3 catalyst caused only 35% of rhenium to be extracted by such treatment. Our results indicate that extraction of 50% of rhenium occurred after calcination at 600°C, but it appeared that it is connected with the support dissolution. The aluminium concentration in the water solution after extraction was about an order of magnitude higher for the catalyst than for bare γ-alumina. These results are in accord with those reported by Schekler- Nahama *et al.* (53) who found, for the first time, that rhenium is extracted together with the aluminum with a (Re/Al) molar ratio of 3. The authors concluded therefore that surface aluminum perrhenate, $Al(ReO_4)_3$, or its decomposition product exists on the surface of the calcined Re/γ-Al_2O_3 catalyst.

The phenomenon of a support dissolution in conditions generally thought to be nonaggressive was also found in the preparation of the MoO_x/γ-Al_2O_3 catalyst (61, 62). The authors reported that during the deposition of ammonium heptamolybdate on γ-alumina by the equilibrium adsorption from an aqueous solution the formation of the ammonium 6-molybdoaluminate salt occurred. The formation of the $[AlMo_6]$ species involved the extraction of Al atoms from the alumina surface. The same species was also present in the solid catalyst after deposition, although its identification was more difficult than that in the liquid phase (61, 62).

Our results indicate that the formation of aluminium perrhenate is expected only during calcination of the Re/γ-Al_2O_3 catalyst at 400–600°C. Bulk phase aluminium perrhenate forms by direct solid–solid reaction between Re_2O_7 and dehydrated Al_2O_3 at 500°C (57) according to the scheme

$$3Re_2O_7 + Al_2O_3 \rightarrow 2Al(ReO_4)_3.$$

Such conditions actually exist during calcination of our samples. The formation of this surface compound may also be expected during the oxidation step of the regeneration procedure of the Pt–Re/Al_2O_3 reforming catalyst, when segregation of Pt and Re occurs (3, 7–10).

Mechanism of oxidation and redispersion of Re supported on γ-Al_2O_3. The mechanism of oxidation and redispersion of Re supported on γ-Al_2O_3 as it appears from the present study is presented in Fig. 9. We start with the catalyst strongly sintered due to high-temperature reduction at 800°C, having nonuniformly distributed Re particles with

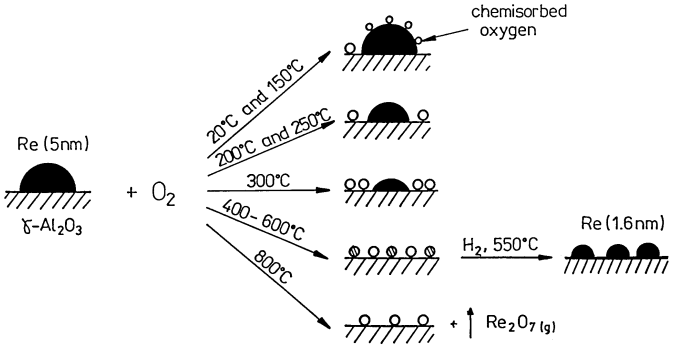

FIG. 9. Schematic presentation of the processes occurring during oxidation and redispersion of the sintered 10.4 wt% Re/γ-Al_2O_3 catalyst.

an average size of about 5 nm. Upon oxidation, depending on the temperature, various chemical and physical processes take place. At 20–150°C dissociative chemisorption of oxygen occurs with the possible formation of a superficial (few monolayers thick) Re oxide. HRTEM images show that already at 150°C some Re_2O_7 is formed, which sublimes and adsorbs on the support. At 200 and 250°C the process of oxidation and sublimation of Re is also detected by measurements of oxygen uptake, though its common interpretation as bulk oxidation is misleading. HRTEM images show clearly that Re particles present in the sample are metallic with no evidence of any surface oxide layer (at least thicker than one or two monolayer). Re_2O_7 molecules from the gas phase dissociate during adsorption on γ-Al_2O_3 into monomeric ReO_4 species. At 300°C measurements of the oxygen uptake suggest complete oxidation of Re to Re_2O_7, but in HRTEM small crystallites of metallic Re are still visible. At 400–600°C ReO_4 species adsorbed on the support form two kinds of a surface compound, probably exhibiting Al–O–ReO_3 and Al–(O–ReO_3)$_3$ structure. This hypothesis is supported by the Raman spectra and the extraction experiments. At 800°C the surface rhenium oxide compounds decompose (especially Al–(O–ReO_3)$_3$) and part of the Re oxide sublimates as Re_2O_7. Due to the high temperature of the alumina support, re-adsorption of the molecules is impossible. Reduction of the catalyst sample oxidised at 500°C in hydrogen at 550°C causes the reduction of the surface Al–O–Re compounds with the formation of uniformly distributed small Re crystallites (redispersion).

CONCLUSIONS

The interaction of the oxygen with the sintered 10.4 wt% Re/γ-Al_2O_3 catalyst is a complex process which depends on the oxidation temperature. At 20–150°C dissociative chemisorption of oxygen occurs with the formation of a supeficial Re oxide, although at 150°C some Re_2O_7 is also present. At 200–300°C the process of Re oxidation accelerates, with instantaneous sublimation of rhenium heptaoxide and its simultaneous adsorption on the support as the ReO_4 species. At 400–600°C, the ReO_4 species forms two kinds of a surface compound with an Al–O–ReO_3 and Al–(O–ReO_3)$_3$ structure. At 800°C the surface aluminum rhenium oxide compounds decompose and in part sublime as Re_2O_7. Mild reduction of the oxidized Re/γ-Al_2O_3 catalyst in H_2 at 550°C causes the redispersion of Re as a 3-fold decrease of the mean particle size of Re and uniform distribution of metallic particles on the support.

ACKNOWLEDGMENTS

The authors thank Professor H. Kubicka for providing the catalyst and for valuable discussions, Dr. M. Wołcyrz for performing XRD measurements, and Mrs. A. Cielecka and Z. Mazurkiewicz for skillful technical assistance.

REFERENCES

1. Olsthoorn, A. A., and Boelhouwer, C., *J. Catal.* **44**, 207 (1976).
2. Mol, J. C., and Moulijn, J. A., *Catal. Sci. Technol.* **8**, 69 (1987).
3. Augustine, S. M., and Sachtler, W. M. H., *J. Catal.* **116**, 184 (1989).
4. Vuurman, M. A., and Wachs, I. E., *J. Phys. Chem.* **96**, 5008 (1992).
5. Vuurman, M. A., Stufkens, D. J., Oskam, A., and Wachs, I. E., *J. Mol. Catal.* **76**, 263 (1992).
6. Kim, D. S., and Wachs, I. E., *J. Catal.* **141**, 419 (1993).
7. Wagstaff, N., and Prins, R., *J. Catal.* **59**, 434 (1979).
8. Mieville, R. L., *J. Catal.* **87**, 437 (1984).
9. Pieck, C. L., Querini, C. A., and Parera, J. M., *Appl. Catal. A* **165**, 207 (1997).
10. Prestvik, R., Moljord, K., Grande, K., and Holmen, A., *J. Catal.* **174**, 119 (1998).
11. Olsthoorn, A. A., and Boelhouwer, C., *J. Catal.* **44**, 197 (1976).
12. Okal, J., Kubicka, H., Kępiński, L., and Krajczyk, L., *Appl. Catal. A* **162**, 161 (1997).
13. Okal, J., and Kubicka, H., *Appl. Catal. A* **171**, 351 (1998).
14. Yao, H. C., and Shelef, M., *J. Catal.* **44**, 392 (1976).
15. Weber, B., and Cassuto, A., *Surf. Sci.* **36**, 81 (1973).
16. Weber, B., Bigeard, B., Mihe, J. P., and Cassuto, A., *J. Vac. Sci. Technol.* **12**, 338 (1975).
17. Fusy, J., Bigeard, B., and Cassuto, A., *Surf. Sci.* **46**, 177 (1974).
18. Ducros, R., Housley, M., and Piquard, G., *Phys. Stat. Sol. (A)* **56**, 187 (1979).
19. Pantel, R., Bujor, R. P. M., and Bardolle, J., *Surf. Sci.* **83**, 228 (1979).
20. Ducros, R., Alnot, M., Ehrhardt, J. J., Housley, M., Piquard, G., and Cassuto, A., *Surf. Sci.* **94**, 154 (1980).
21. Ducros, R., and Fusy, J., *J. Electron Spectrosc. Rel. Phenom.* **42**, 305 (1987).
22. Zaera, F., and Somorjai, G. A., *Surf. Sci.* **154**, 303 (1985).
23. Tysoe, W. T., Zaera, F., and Somorjai, G. A., *Surf. Sci.* **200**, 1 (1988).
24. Menon, P. G., Sieders, J., Streefkerk, F. J., and van Keulen, G. J. M., *J. Catal.* **29**, 188 (1973).
25. Bolivar, C., Charcosset, H., Frety, R., Primet, M., Tournayan, L., Betizeau, C., Leclerq, G., and Maurel, R., *J. Catal.* **45**, 163 (1976).
26. Paryjczak, T., Gebauer, D., and Kozakiewicz, A., *J. Colloid Interface Sci.* **70**, 320 (1979).
27. Eskinazi, V., *Appl. Catal.* **4**, 320 (1982).
28. Isaacs, B. H., and Petersen, E. E., *J. Catal.* **85**, 1, 8 (1984).
29. Chądzyński, G. W., and Kubicka, H., *Thermochim. Acta.* **158**, 369 (1990).
30. Pieck, C. L., Marecot, P., Parera, J. M., and Barbier, J., *Appl. Catal. A* **126**, 153 (1995).
31. Pieck, C. L., Marecot, P., Querini, C. A., Parera, J. M., and Barbier, J., *Appl. Catal. A* **133**, 281 (1995).
32. Cimino, A., De Angelis, B. A., Gazzoli, D., and Valigi, M., *Z. Anorg. Allg. Chem.* **460**, 86 (1980).
33. Peaock, R. D., *in* "Comprehensive Inorganic Chemistry" (I. C. Bailar, H. J. Emeleus, R. Nyholm, and A. F. Trotman-Dickenson, Eds.), p. 905. Pergamon Press, London, 1973.
34. Xiaoding, Xu., Boelhouver, C., Benecke, J. J., Vonk, D., and Mol, J. C., *J. Chem. Soc., Faraday Trans. 1.* **82**, 1945 (1986).
35. Maksimov, Y. V., Kushnerev, M. Y., Dumesic, J. A., Nechitailo, A. E., and Fridman, R. A., *J. Catal.* **45**, 114 (1976).
36. Arnoldy, P., Van Oers, E. M., Bruinsma, O. S. L., De Beer, V. H. J., and Moulijn, J. A., *J. Catal.* **93**, 231 (1985).
37. Edreva-Kardjieva, R. M., and Andreev, A. A., *J. Catal.* **94**, 97 (1985).
38. Laiyuan, Ch., Yuegin, N., Jingling, Z., Liwu, L., Xihui, L., and Sen, Ch., *J. Catal.* **145**, 132 (1994).
39. Sibeijn, M., Van Veen, J. A. R., Bliek, A., and Moulijn, J. A., *J. Catal.* **145**, 416 (1994).
40. Turek, A. M., Wachs, I. E., and De Canio, E., *J. Phys. Chem.* **96**, 5000 (1992).

41. Spronk, R., Van Veen, J. A. R., and Mol, J. C., *J. Catal.* **144**, 472 (1993).
42. Kawai, T., Jiang, K. M., and Ishikawa, T., *J. Catal.* **159**, 288 (1996).
43. Kerkhof, F. P. J. M., Moulijn, J. A., and Thomas, R., *J. Catal.* **56**, 279 (1979).
44. Wang, L., and Hall, W. K., *J. Catal.* **82**, 177 (1983).
45. Nacheff, M. S., Kraus, L. S., Ichikawa, M., Hoffman, B. M., Butt, J. B., and Sachtler, W. M. H., *J. Catal.* **106**, 263 (1987).
46. Engels, S., Lausch, H., and Meiners, H. W., *React. Kinet. Catal. Lett.* **44**, 251 (1991).
47. Shpiro, E. S., Avaev, V. I., Antoshin, G. V., Ryashentseva, M. A., and Minachev, K. M., *J. Catal.* **55**, 402 (1978).
48. Kirlin, P. S., Strohmeier, B. R., and Gates, B. C., *J. Catal.* **98**, 308 (1986).
49. Kerkhof, F. P. J. M., and Moulijn, J. A., *J. Phys. Chem.* **83**, 1613 (1979).
50. Hietala, J., Root, A., and Knuuttila, P., *J. Catal.* **150**, 46 (1994).
51. Stolarek, G., and Wrzyszcz, J., *Chem. Stosow.* **20**, 297 (1976).
52. Valigi, M., and Minelli, G., *J. Less Common Metals.* **51**, 271 (1977).
53. Schekler-Nahama, F., Clause, O., Commereuc, D., and Saussey, J., *Appl. Catal. A* **167**, 247 (1998).
54. Kubicka, H., and Okal, J., *React. Kinet. Catal. Lett.* **48**, 195 (1992).
55. Kubicka, H., *Roczniki Chem.* **47**, 599 (1973).
56. Krebs, B., Muller, A., and Beyer, H. H., *Inorg. Chem.* **8**, 436 (1969).
57. Baud, G., and Capestan, M., *Bull. Soc. Chim. Fr.* **11**, 3608 (1966).
58. Peeters, I., Van der Gon, A. W. D., Reijme, M. A., Kooyman, P. J., De Jong, A. M., Van Grondelle, J., Brongersma, H. H., and Van Santen, R. A., *J. Catal.* **173**, 28 (1998).
59. Reardon, J., Datye, A. K., and Soult, A. G., *J. Catal.* **173**, 145 (1998).
60. Mulcahy, F. M., Fay, M. J., Proctor, A., Houalla, M., and Hercules, D. M., *J. Catal.* **124**, 231 (1990).
61. Carrier, X., Lambert, J. F., and Che, M., *J. Am. Chem. Soc.* **119**, 10137 (1997).
62. Le Bihan, L., Blanchard, P., Fournier, M., Grimblot, J., and Payen, E., *J. Chem. Soc., Faraday Trans.* **94**(7), 937 (1998).